ELSEVIER

Biophysical Chemistry 98 (2002) 93–104

Biophysical Chemistry

www.elsevier.com/locate/bpc

Effects of inert volume-excluding macromolecules on protein fiber formation. I. Equilibrium models

Damien Hall, Allen P. Minton*

Section on Physical Biochemistry, Laboratory of Biochemistry and Genetics, National Institute of Diabetes and Digestive and Kidney Diseases, National Institutes of Health, Bethesda, MD, USA

Received 1 October 2001; received in revised form 13 November 2001; accepted 13 November 2001

Abstract

The equilibrium Oosawa–Asakura model for nucleated assembly of rod-like protein fibers is recast in terms of dimensionless (scaled) quantities. The model is then generalized to treat arbitrarily large deviations from thermodynamic ideality arising from high fractional volume occupancy by an inert protein or polymer. Each state of association of the self-associating protein is modeled as an equivalent rigid convex particle (sphere or spherocylinder) and the crowding species is modeled either as an equivalent sphere or cylindrical rod. The resulting conservation of mass relation is readily solved to yield the fractional abundance of monomer, from which the entire equilibrium distribution of oligomeric species can be calculated, either directly or through the use of an additional scaling relationship. Results indicating the potential effect of volume occupancy on the equilibrium solubility of the self-associating protein and upon the equilibrium distribution of polymer size are presented. It is found that the fractional (logarithmic) change in both solubility and in the breadth of the polymer size distribution scale almost linearly with the fractional (logarithmic) change in the thermodynamic activity of monomer.

Keywords: Protein assembly; Macromolecular crowding; Excluded volume; Thermodynamic nonideality

1. Introduction

The reversible formation of fibrous aggregates of protein is widespread in biology [1]. Although all physiological fluid media are characterized by a high total macromolecular concentration, the effect of high total macromolecular concentration on the rate and/or extent of protein fiber formation has been studied systematically only in the cases of deoxy sickle hemoglobin [2,3], actin [4] and the bacterial septation protein FtsZ [5]. While the detailed mechanism of fiber assembly differs between each of these proteins, in all three cases it has been shown that the large effect of high protein concentration on the rate and/or extent of polymer formation may be essentially entirely accounted for on the basis of excluded volume. On the basis of these studies, one would expect excluded volume to play a significant role in most or all reactions leading to protein fiber formation under physiological conditions.

Since the detailed mechanism of fiber formation varies between different proteins and perhaps between different experimental conditions for a

*Corresponding author. Building 8, Room 226, NIH, Bethesda, MD 20892-0830, USA. Tel.: +1-301-496-3604; fax: +1-301-402-0240.

E-mail address: minton@helix.nih.gov (A.P. Minton).

0301-4622/02/$ - see front matter
PII: S0301-4622(02)00087-X

single protein as well, and in view of the amount of work involved in the characterization of a polymerizing system, it is unlikely that a large number of different fiber-forming systems will be exhaustively characterized experimentally. We therefore attempt to determine whether there exist general qualitative or semiquantitative relationships governing excluded volume effects upon the rate and extent of protein fiber formation that are independent of, or insensitive to, detailed differences in reaction mechanism.

In the present paper, we generalize the Oosawa–Asakura equilibrium model for nucleated fiber formation [1,6] to take into account the thermodynamic consequences of excluded volume arising from the presence of high concentrations of inert macromolecules. Analytic and numeric solutions of the quantitative relations obtained reveal general features of the simulated polymerization equilibria that are insensitive to details of the model, and hence likely to apply to more complex and realistic processes as well.

2. Theory

2.1. Equilibrium relations

All of the models to be considered in the present work are simplifications of a general equilibrium model for self-association, in which the equilibrium constant for addition of monomer to an oligomer of degree of polymerization (dop) $i-1$ is defined as

$$K_i(M^{-1}) = \frac{c_i}{c_{i-1}c_1} \tag{1}$$

where c_i denotes the molar concentration of i-mer. This formalism is valid under thermodynamically nonideal as well as thermodynamically ideal conditions, recognizing that

$$K_i = K_i^0 \Gamma_i(\{c\}) \tag{2}$$

where K_i^0 is the value of K_i in the ideal limit. Γ_i is a nonideal correction factor given by

$$\Gamma_i(\{c\}) \equiv \frac{\gamma_{i-1}(\{c\})\gamma_1(\{c\})}{\gamma_i(\{c\})} \tag{3}$$

where γ_j denotes the thermodynamic activity coefficient of species j, and $\{c\}$ denotes the total solute composition, including concentrations of solutes other than the self-associating protein [7,8]. In the present work we consider only situations in which the self-associating protein is itself dilute; deviations from ideality are attributed exclusively to the presence of other macromolecular species at high concentration. Under these conditions the γ_i and K_i will be independent of the concentration of polymerizing protein.

We define the (dimensionless) mass fraction of i-mer as

$$f_i = \frac{ic_i}{c_{\text{tot}}} \tag{4}$$

where c_{tot} denotes the total concentration of protein expressed as moles of monomer or protomer per liter

$$c_{\text{tot}} = \sum_{i=1}^{\infty} ic_i \tag{5}$$

We additionally define the (dimensionless) scaled equilibrium constant

$$X_i \equiv K_i c_{\text{tot}} = X_i^0 \Gamma_i \tag{6}$$

where X_i^0 is the value of X_i in the ideal limit. Combining Eqs. (1) and (4) and Eq. (6), we obtain the following set of scaled (dimensionless) equilibrium relations

$$\frac{f_i}{f_{i-1}f_1} = \frac{i}{i-1}X_i \tag{7}$$

By recursive application of Eq. (7), it may be shown that

$$f_i = i\Phi_i f_1^i \tag{8}$$

where Φ_i is a dimensionless cumulative equilibrium constant given by

$$\Phi_i = \prod_{j=2}^{i} X_j \tag{9}$$

Conservation of mass is expressed by the following relation

$$1=\sum_{i=1}^{\infty} f_i = f_1 + \sum_{i=2}^{\infty} i\Phi f_1^i \qquad (10)$$

Given the values of X_i, Eq. (9) and Eq. (10) may be solved—in principle—for the value of f_1, and thence, via Eq. (8), the values of all f_i. If the infinite series indicated in Eq. (10) is not rapidly convergent, numerical solution may be difficult or impractical. However, the problem may be simplified considerably, without significant sacrifice of physical relevance, as described below.

2.2. Simplified structural/energetic model for nucleated fiber formation

It is assumed, in accordance with the Oosawa–Asakura model, that there exists some smallest oligomeric species containing all elements of the periodic structure characterizing the fully formed protein fiber, and that addition of monomer to oligomers of this size or larger (under thermodynamically ideal conditions) is associated with equal increments of free energy, i.e. an equal stepwise association equilibrium constant. We shall subsequently refer to this particular oligomer as 'nucleus', with degree of polymerization n, species with degree of polymerization $\leqslant n$ as 'prenuclear' species, and species with degree of polymerization $>n$ as 'postnuclear' species. According to this simplification $K_i^0 = K_\infty^0$ and $X_i^0 = X_\infty^0$ for $i>n$. It is further assumed that the nucleus represents a 'starting point' or scaffold for construction of a fiber, according to which the radius of the fiber is fixed. Thus, addition of monomer to oligomers of dop n or greater results in fiber elongation, but does not alter the radius of the fiber.

Previous studies of nucleated fiber formation [1,9] have postulated that the equilibrium association constant for formation of prenuclear oligomers is independent of i for $i=2-n$, even though there is no obvious reason to expect a priori that stepwise entropy changes associated with the addition of monomer to small oligomers are uniform [10]. For the sake of comparison with these previous models we define a single prenuclear stepwise association constant K_{pre}^0, equal to the $(n-1)$th root of $\prod_{j=2}^{n} K_j^0$, and the corresponding normalized prenuclear association constant X_{pre}^0. Hence in the ideal limit, the simplified equilibrium model for nucleated fiber formation reduces to Eq. (7) with $X_i = X_{\mathrm{pre}}^0$ for $i \leqslant n$, and $X_i = X_\infty^0$ for $i>n$.

2.3. Hard particle models for excluded volume

In the present study it is stipulated that excluded volume effects arise from the presence of a single species of inert macromolecule (called C or 'crowder') that may occupy a substantial fraction of the total volume of the fluid medium. The fiber-forming protein (called A) is assumed to be dilute, contributing negligibly to the fractional volume occupancy of the medium. Thus, the thermodynamic activity coefficient of each species of A is independent of all f_j and, for a specified molecular geometry, depends only upon the concentration of crowder.

The contribution of excluded volume to the thermodynamic activity of a macrosolute is calculated using approximate equations of state derived for hard particle fluids, in which each molecular species is represented by an equivalent hard particle having a size and shape resembling that of the corresponding macromolecule (insofar as possible). Justification for this procedure has been presented elsewhere [11]. In the present study we employ the following equivalent particles, shown schematically in Fig. 1.

(1) Monomers and oligomers of A with dop i, where $1 \leqslant i \leqslant n$, are represented as equivalent spheres with a volume equal to i times that of monomer. The radius of the spherical particle is thus given by

$$r_i = i^{1/3} r_1 \qquad (11)$$

(2) Rod-like oligomers of A with dop $i>n$ are represented as spherocylinders[1] with a volume equal to i times that of monomer and a (constant) cylindrical radius equal to r_n, the radius of the spherical nucleus. The ratio of the length of the cylindrical portion of the spherocylinder to its diameter is then given by the following relation-

[1] A spherocylinder is a cylinder capped on each end by a hemisphere.

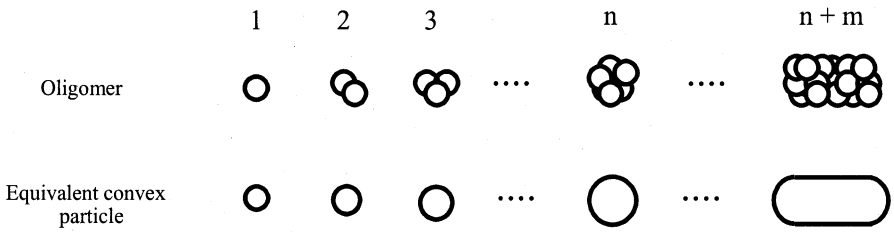

Fig. 1. Schematic representation of self-associating tracer protein A as a monomer, prenuclear and nuclear oligomers ($1<i\leqslant n$), and postnuclear rod-like oligomer ($i=n+m$, where $m>0$).

ship obtained from considerations of conservation of volume

$$L_i = \frac{2}{3n}(i-n) \tag{12}$$

(3) Crowder molecules are modeled according to the structure of the crowder. A rigid globular protein is represented by an equivalent hard spherical particle with radius r_C, and a large random-coil polymer is represented by a random lattice of cylindrical rods with radius r_C. According to the scaled particle theory of Cotter [12], the activity coefficient of a spherocylindrical tracer with cylindrical radius r_T and cylindrical length/diameter ratio L_T in a fluid of rigid spheres occupying fraction φ of total fluid volume is given by

$$\ln\gamma_T = -\ln(1-\varphi) + A_1 Q + A_2 Q^2 + A_3 Q^3 \tag{13}$$

where

$$Q = \varphi/(1-\varphi)$$
$$A_1 = R^3 + 3R^2 + 3R + 1.5L_T(R^2 + 2R + 1)$$
$$A_2 = 1.5(2R^3 + 3R^2) + 4.5L_T(R^2 + R)$$
$$A_3 = 3R^3 + 4.5L_T R^2$$

and

$$R \equiv r_T/r_C.$$

In the limiting case of a spherical tracer ($L_T = 0$), Eq. (13) reduces to an earlier result obtained for rigid sphere mixtures [13].

According to the available volume theory of Giddings et al. [14], the activity coefficient of a spherocylindrical tracer particle in a fluid of rigid rods of radius r_C occupying fraction φ of total fluid volume is given by

$$\ln\gamma_T = \left(1 + \frac{r_T}{r_C}\right)\left(1 + (L_T + 1)\frac{r_T}{r_C}\right)\varphi \tag{14}$$

In the limiting case of a spherical tracer ($L_T = 0$), Eq. (14) reduces to the result obtained for the case of a sphere in a random matrix of rods by Ogston [15].

For both hard particle models, the excluded volume effect will then be specified by two input parameters, φ, the volume fraction of crowder, and $R \equiv r_1/r_C$, where r_1 is the radius of monomer and r_C is either the radius of a hard sphere crowder or the cylindrical radius of a hard rod crowder.

In Appendix A it is shown that for both excluded volume models, Γ_i is independent of i, and therefore denoted henceforth by Γ_∞, for all $i>n$. It follows that for all $i>n$, the value of $X_i = K_i^0 \Gamma_i c_{tot}$ is likewise independent of i, and will be denoted here by X_∞. Eq. (9) may then be rewritten as

$$\Phi_i = \Phi_n X_\infty^{i-n} \tag{15}$$

and the conservation of mass condition Eq. (10) thus becomes

$$1 = f_1 + \sum_{i=2}^{n} i\,\Phi_i f_1^i + \Phi_n f_1^n \sum_{j=1}^{\infty} (n+j)[X_\infty f_1]^j \tag{16}$$

The last term on the r.h.s. of Eq. (16), representing the total mass fraction of all oligomers with dop exceeding n, will subsequently be termed the mass fraction of polymer and denoted by

f_{poly}. The infinite series appearing in this term may be analytically evaluated [16], leading to

$$1 = f_1 + \sum_{i=2}^{n} i\Phi_i f_1^i + \Phi_n f_1^n \left[n\frac{X_\infty f_1}{1 - X_\infty f_1} + \frac{X_\infty f_1}{(1 - X_\infty f_1)^2} \right] \quad (17)$$

Eq. (17) may be recast as a polynomial in f_1 of order n, which has one and only one physical root (i.e. a real root lying between 0 and the lesser of 1 or $1/X_\infty$). This root may be readily evaluated by any of a number of polynomial-solving algorithms [17]. Given the physical value of f_1 satisfying Eq. (17), the weight-average degree of polymerization, denoted by dop_w may be evaluated as follows:

$$\begin{aligned} dop_w &= \sum_{i=1}^{\infty} i f_i = f_1 + \sum_{i=2}^{\infty} i^2 \Phi_i f_1^i \\ &= f_1 + \sum_{i=2}^{n} i^2 \Phi_i f_1^i + \sum_{i=n}^{\infty} i^2 \Phi_i f_1^i \\ &= f_1 + \sum_{i=2}^{n} i^2 \Phi_i f_1^i + \Phi_n f_1^n \sum_{j=1}^{\infty} (n+j)^2 (X_\infty f_1)^j \\ &= f_1 + \sum_{i=2}^{n} i^2 \Phi_i f_1^i + \Phi_n f_1^n \left[n^2 \frac{X_\infty f_1}{1 - X_\infty f_1} + 2n \frac{X_\infty f_1}{(1 - X_\infty f_1)^2} + \frac{X_\infty f_1 + (X_\infty f_1)^2}{(1 - X_\infty f_1)^3} \right] \end{aligned} \quad (18)$$

It will be shown subsequently that equilibrium species distributions characteristic of nucleated fiber formation contain a low dop fraction consisting primarily of monomer and a high dop fraction which may be separated from the low dop fraction by centrifugation. We shall therefore refer to the total fractional mass of all species with $dop \leqslant n$ ($\sum_{i=1}^{n} f_i$) as the soluble fraction, f_{sol}, and the remainder ($\sum_{i=n+1}^{\infty} f_i$) as the fraction of 'polymer', f_{poly}.

2.4. Scaling relationships

It follows from Eq. (8) and Eq. (15) that, for i and $j > n$,

$$\frac{f_i}{f_j} = \frac{i}{j}\,\Theta^{i-j} \quad (19)$$

where $\Theta \equiv X_\infty f_1$. Consider two different sets of experimental conditions (condition sets 1 and 2) in which the various X_i characterizing the self-associating system, including X_∞, have different values denoted $X_i^{(1)}$ and $X_i^{(2)}$. These different values of X_i will lead to two different solutions of Eq. (17), denoted $f_1^{(1)}$ and $f_1^{(2)}$, respectively, two different values of Θ, denoted Θ_1 and Θ_2, respectively, and result in two different values of f_{poly}, denoted by $f_{poly}(\Theta_1)$ and $f_{poly}(\Theta_2)$, respectively. For condition sets 1 and 2 we may respectively write

$$\frac{f_i}{f_j} = \frac{i}{j}\,\Theta_1^{i-j} \quad (20)$$

and

$$\frac{f_m}{f_n} = \frac{m}{n}\Theta_2^{m-n} \quad (21)$$

Inspection of Eq. (20) and Eq. (21) reveals that f_m/f_n will be identical to f_i/f_j, if $m = ci$, $n = cj$, and $\Theta_2 = \Theta_1^{(1/c)}$. Put another way, given any two values for Θ_1 and Θ_2, there exists a scaling factor $c \equiv \ln(\Theta_1)/\ln(\Theta_2)$ such that the ratio of mass fractions of oligomers of dop i and dop j under condition set 1 is the same as the ratio of mass fractions of oligomers of dop ci and dop cj under condition set 2. Thus, variation in the value of Θ (i.e. in the value of c) leads to an expansion ($c > 1$) or contraction ($c < 1$) of the width of the distribution by a factor of c, but does not affect the ratio of relative abundances of (ci)-mer and (cj)-mer. Since the total mass fraction of polymer in each distribution must scale as the relative width

times the relative height of that distribution, it follows that

$$\frac{cf_{ci}(\Theta_2)}{f_i(\Theta_1)} = \frac{f_{\text{poly}}(\Theta_2)}{f_{\text{poly}}(\Theta_1)} \tag{22}$$

Eq. (22) is a universal relationship that depends only upon the validity of the assumption that X_i is independent of i for all $i > n$. It applies between any two distributions of oligomers, independent of the values of n, X^0_∞, or Γ_∞, so long as comparisons are restricted to postnuclear species only. Given one distribution of postnuclear species and the associated values of Θ and f_{poly}, it becomes trivially simple to compute any other distribution of postnuclear species via Eq. (22), given the corresponding values of Θ and f_{poly}.[2]

2.5. Method of calculation

The ideal model is specified by three input parameters, n, X^0_{pre}, and X^0_∞. Given the values of these three parameters, the values of f_1 and $\Theta(\equiv X^0_\infty f_1)$ are calculated for $\varphi = 0$ via numerical solution of Eq. (17), which enables the subsequent calculation of f_{sol} and dop_w as described above. We shall refer to these particular values of f_1 and Θ as the ideal or reference values and denote them by f_1^0 and Θ^0. The excluded volume contribution to nonideal behavior is specified by two additional input parameters, $\varphi(>0)$ and R. Given these parameters, the values of γ_i are then calculated for $i = 1-n+1$ using either Eq. (13) or Eq. (12) depending upon the choice of crowder model. Then Γ_i and X_i are calculated as described above for $i = 1$ to $n+1$, X_∞ set equal to X_{n+1}, and Eq. (17) is again solved for f_1 and Θ, which differ from the respective reference values. The values of f_{sol} and dop_w are calculated as before, together with the scaling factor $c = \ln(\Theta^0)/\ln(\Theta)$, which indicates the expansion of the distribution of postnuclear species relative to that calculated for the same parameters under ideal conditions ($\varphi = 0$). The distribution of postnuclear species may be calculated either via repeated application of Eq. (7), when the distribution is sufficiently narrow, or via the scaling relation, Eq. (22), when the distribution is too broad to make direct calculation impractical.

Numerical calculations were performed using MATLAB 5.3 (Mathworks, Natick, MA). Copies of the scripts used are available upon request.

3. Results and discussion

The equilibrium properties of the simplified model for nucleated fiber formation described here have been explored in the ideal limit by Oosawa et al. [1,6] and by Goldstein and Stryer [9]. The nucleated model differs qualitatively in the predicted distribution of species from that predicted by simple linear models for fiber formation, such as the isodesmic [18], isoenthalpic [10], or quasi-isodesmic [19] models. In the linear model the distribution has a single maximum corresponding to either monomer, or some very high dop, depending upon the total concentration of protein relative to the equilibrium association constant(s). The equilibrium distribution of species calculated according to the (ideal) Oosawa–Asakura model is quite sensitive to the ratio $\sigma \equiv X_{\text{pre}}/X_\infty$ $(= X^0_{\text{pre}}/X^0_\infty)$, termed the cooperativity factor by Goldstein and Stryer [9]. When $\sigma = 1$, the Oosawa–Asakura model reduces to the isodesmic model. However, when σ becomes significantly less than unity, a bimodal distribution is predicted, consisting of a narrow range of low dop species, with a maximum at monomer, and a second very broad and shallow distribution with a maximum at high dop. Calculated examples are shown in the left and center panels of Fig. 2.

Given the above specification of the relative sizes and shapes of all species, the sedimentation coefficient of each oligomer relative to that of monomer may be calculated using approximate relations given in Appendix B. The cumulative fraction of protein with a sedimentation coefficient below a given value, denoted by f_{cum}, is plotted

[2] For purposes of calculation of the species index, ci is rounded to the nearest integer. The accuracy of this approximation has been checked by comparison of distributions calculated directly using Eq. (7) and Eq. (8) and calculated indirectly via Eq. (22). It is recognized that Eq. (22) only permits one to calculate the abundance of every cth dop, rather than every dop. However, this is sufficient for all practical purposes.

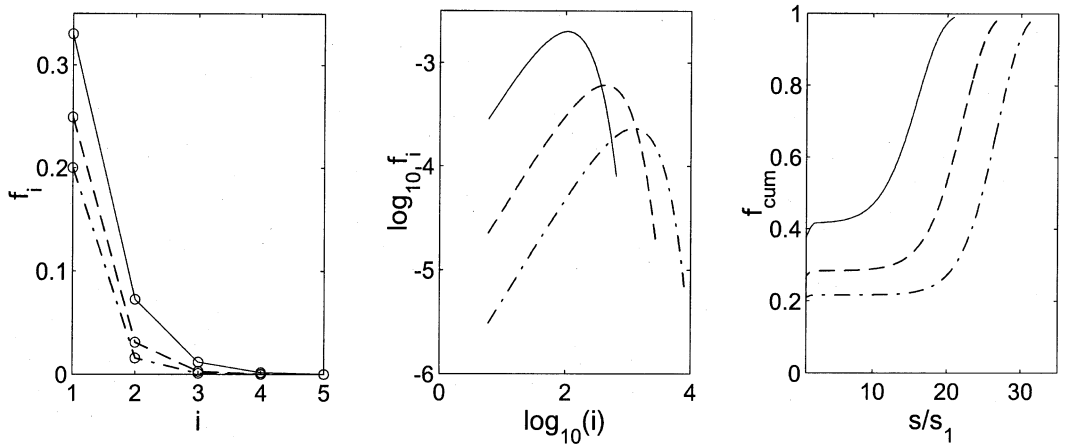

Fig. 2. Distributions of oligomer size and sedimentation coefficient, calculated in the ideal limit for $n=5$ and several combinations of pre- and post-nuclear equilibrium association constants. Solid curves: $X^0_{pre}=0.333$, $X^0_\infty=3$; long dashed curves: $X^0_{pre}=0.25$, $X^0_\infty=4$; dot-dashed curves: $X^0_{pre}=0.2$, $X^0_\infty=5$; Left panel: distribution of prenuclear oligomers. Center panel: distribution of postnuclear oligomers. Right panel: cumulative distribution of sedimentation coefficient. f_{cum} denotes the cumulative amount of protein with sedimentation coefficient less than or equal to the indicated relative sedimentation coefficient.

for each of the calculated distributions shown in the right panel of Fig. 2. In each case, the presence of a plateau region with f_{cum} equal to the sum of mass fractions of prenuclear species indicates that under these conditions, it is relatively simple to separate slowly sedimenting species ($dop \leqslant n$) and rapidly sedimenting species ($dop > n$) species via centrifugation. We thus operationally refer to the protein in the slowly sedimenting fraction (mostly monomer) as 'soluble' protein, and the protein in the rapidly sedimenting fraction ($dop > n$) as 'polymer'. It may be seen that the solubility (mass fraction of soluble protein) and weight-average degree of polymerization are sensitive functions of n, X^0_{pre} and X^0_∞.

An example of the possible effect of excluded volume on the distribution of oligomeric species is shown in Fig. 3. The results shown were obtained for a single set of ideal parameters, given in the figure caption, upon varying the total volume fraction of an inert hard spherical crowding protein equal in size to that of the monomer. It may be seen that upon increasing the fractional occupancy of crowder from 0 to 0.3, the solubility decreases approximately 50-fold (left panel) and the distribution of postnuclear oligomers expands by a factor of approximately 100-fold (center panel). The right hand panel shows that the shape of the distribution of postnuclear oligomers is conserved upon normalization relative to the maximal fractional abundance, as predicted by the scaling relation Eq. (22).[3] More generally, it is possible to show that for both the rigid sphere and rigid rod crowder models, an increase in the fractional occupancy φ results in a decrease in X_{pre}/X_∞, i.e. an increase in the cooperative nature of the assembly process, for all $R>0$ and $n \geqslant 2$.[4]

While the magnitude of excluded volume effects increases monotonically with increasing total fractional volume occupancy φ, the relationship is highly nonlinear, and moreover depends sensitively upon the relative sizes of crowder and tracer species [7,8,11]. We hypothesized that there may be a more straightforward relationship between the magnitude of one excluded volume effect and a second excluded volume effect, namely the effect of crowder on the activity coefficient of monomer. The hypothesis is tested by plotting fractional changes in solubility and the scaling parameter c

[3] Although the total amount of polymer increases with increasing volume occupancy, the maximum amplitude of the distribution decreases due to the distribution of protein among a rapidly increasing number of states of oligomerization.

[4] Calculations available upon request.

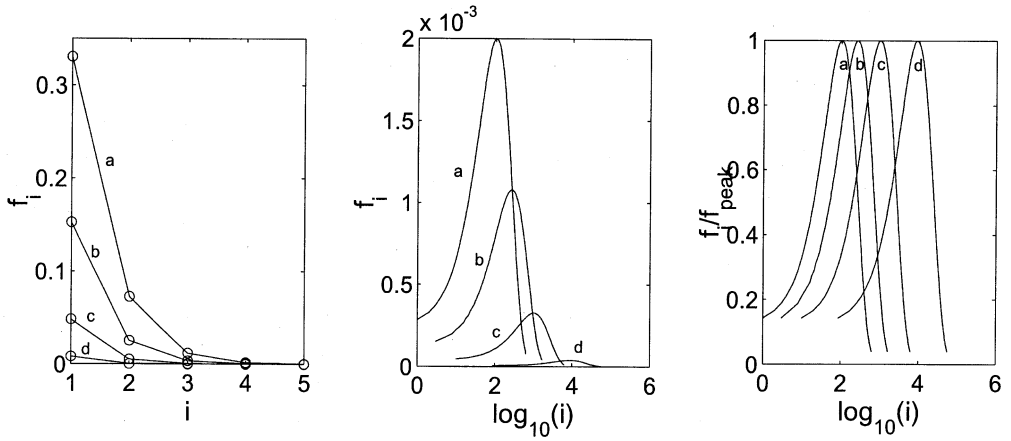

Fig. 3. Distributions of oligomer size, calculated for $n=5$, $X^0_{pre}=0.333$, $X^0_\infty=3$, and $r_1=r_C$. Curves calculated for $\varphi=0$ (a); 0.1 (b); 0.2 (c); and 0.3 (d). Right panel shows same data as center panel, normalized to the maximum amplitude of the distribution of postnuclear species.

against the activity coefficient of monomer, and exploring the extent to which the correlation between the two plotted variables depends upon the particulars of the simulation. A selection of results obtained is presented in Fig. 4 and Fig. 5. Several salient points emerge from these results and comparable results obtained for other values of n and R (data not shown, but available upon request).

(1) When the value of X^0_∞ becomes sufficiently great, the logarithm of each of the three variables examined (the scaling factor c, the relative solubility f_{sol}/f^0_{sol}, and the relative activity of monomer a_1/a^0_1) vs. approaches a limiting quasi-linear dependence upon the logarithm of the activity coefficient of monomer. The average slope of this quasi-linear dependence is almost entirely independent of the values of X^0_{pre}, X^0_∞, and R (the ratio of monomer to crowder size), but increases, in an absolute sense, with increasing n.

(2) The (average) slope of the limiting quasi-linear dependence of both $\log f_{sol}/f^0_{sol}$ and $\log a_1/a^0_1$ upon $\log \gamma_1$ is essentially identical for the case of the crowder modeled as a rigid sphere and for the case of the crowder modeled as a rigid rod. However, for larger values of n, the limiting slope of $\log c$ vs. $\log \gamma_1$ is larger for the spherical crowder model than for the rod-like crowder model.

(3) To the extent that species intermediate between monomer and large rod-like aggregates are absent, one would expect the formation of long fibers to be thermodynamically analogous to condensation. It is assumed in the conventional treatment of condensation (or solubility) that the thermodynamic activity of the solute in equilibrium with the condensed phase is independent of the amount or size of condensed phase, from which it follows that the thermodynamic activity of monomer in equilibrium with the condensed phase should be constant at constant temperature [20]. The observation that a_1 increases with increased crowding appears to be at variance with this expectation. However, there is a simple explanation of this apparent anomaly. Under conditions such that the weight-average dop is very large, Eq. (18) tells us that $X_\infty f_1=X^0_\infty \Gamma_\infty f_1\approx 1$. It follows that

$$\begin{aligned}\ln a_1(\varphi) &= \ln\gamma_1(\varphi)+\ln f_1(\varphi)+\ln c_{tot}\\ &\approx \ln\gamma_j(\varphi)-\ln\gamma_{j-1}(\varphi)-\ln X^0_\infty\\ &+\ \ln c_{tot}\end{aligned} \tag{23}$$

where γ_{j-1} and γ_j denote the activity coefficients of any two oligomers such that $j>n+1$. Denoting

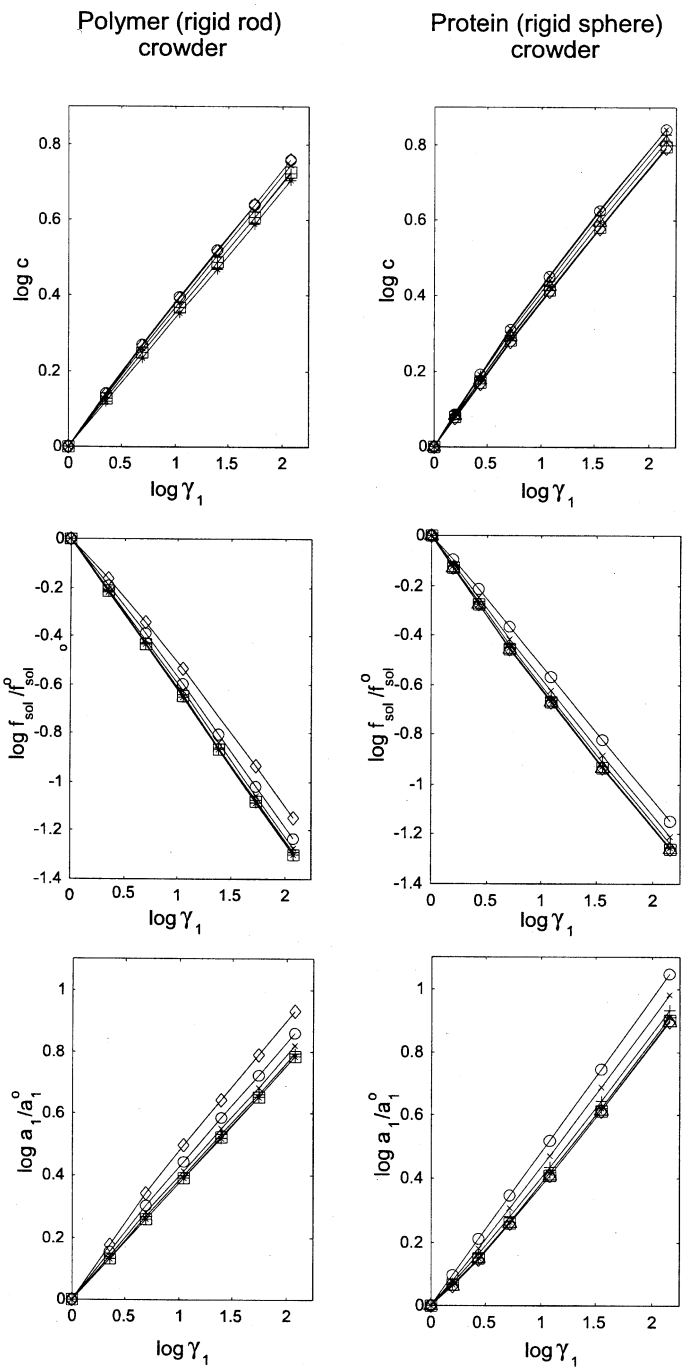

Fig. 4. Log c, log f_{sol}/f^0_{sol} and log a_1/a^0_1 plotted as a function of log γ_1. Results in panels on left side of figure were calculated using rigid rod model of crowder, results in panels on right hand side were calculated using rigid sphere model of crowder. Families of curves plotted in each panel were calculated with $n=2$ and the following combinations of X^0_{pre} and X^0_∞: {0.5, 2}, {0.333, 3}, {0.2, 5}, {0.1, 10}, and {0.0333, 30}. Curves lying furthest from the consensus curve were obtained for the smallest values of X^0_∞.

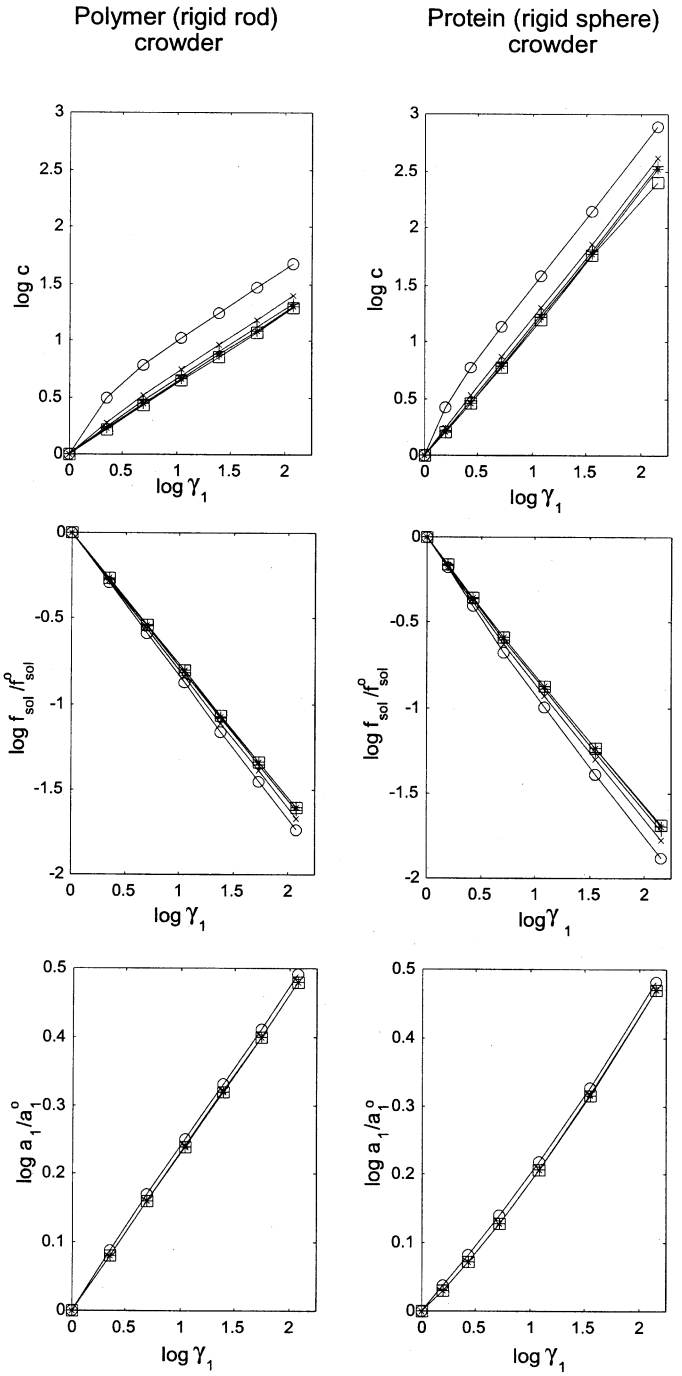

Fig. 5. Same as Fig. 4, except results were obtained with $n=7$.

the value of a_1 at $\varphi=0$ by a_1^0, it follows from Eq. (23) that

$$\ln\frac{a_1}{a_1^0}\approx\ln\gamma_j(\varphi)-\ln\gamma_{j-1}(\varphi)=g(\varphi) \tag{24}$$

It is shown in Appendix A that $g(\varphi)$ is independent of the value of j, and moreover, for the model of crowder as a hard rod, linear in φ. It is thus evident that the activity of protein in the 'condensed' and solution phases can be regarded as a constant only under conditions of constant excluded volume (i.e. constant crowder concentration).

(4) The results presented in Fig. 4 and Fig. 5 indicate a linear or near-linear dependence of solubility on $\log\gamma_1$. Since the model of crowder as a hard rod predicts that $\log\gamma_1$ varies linearly with φ [Eq. (14)], these results predict a linear dependence of the logarithm of the solubility upon the concentration of polymeric crowder, in accordance with published observations [21–23].

Work is currently in progress on the extension of the models presented above to treat the effect of excluded volume due to high volume occupancy of an inert crowding species on kinetics of assembly of protein fibers.

Appendix A: Calculation of Γ_i for $i>n$

Hard sphere crowder. According to Eq. (13) [12],

$$\begin{aligned}\ln\Gamma_i&=\ln\gamma_1+\ln\gamma_{i-1}-\ln\gamma_i\\&=\ln\gamma_1+[A_1^{(i-1)}-A_1^{(i)}]Q\\&\quad+[A_2^{(i-1)}-A_2^{(i)}]Q^2+[A_3^{(i-1)}-A_3^{(i)}]Q^3\end{aligned} \tag{A1}$$

where $A_j^{(i)}$ denotes the value of A_j corresponding to species i. For all $i>n$, the addition of a monomer to an oligomer results in an increase in L by a constant increment Δ, with no change in R. Thus, $L^{(i)}=L^{(i-1)}+\Delta$, and

$$\begin{aligned}A_1^{(i)}&=A_1^{(i-1)}+1.5\Delta(R^2+2R+1)\\A_2^{(i)}&=A_2^{(i-1)}+4.5\Delta(R^2+R)\\A_3^{(i)}&=A_3^{(i-1)}+4.5\Delta R^2\end{aligned} \tag{A2}$$

Combination of Eq. (A1) and Eq. (A2) yields

$$\begin{aligned}\ln\Gamma_i&=\ln\gamma_1-1.5\Delta(R^2+2R+1)Q\\&\quad-4.5\Delta(R^2+R)Q^2-4.5\Delta R^2Q^3\end{aligned} \tag{A3}$$

which is independent of i.

Hard rod crowder. According to Eq. (14) [14],

$$\ln\Gamma_i=\ln\gamma_1+\left(1+\frac{r_i}{r_C}\right)(L^{(i-1)}-L^{(i)})\frac{r_i}{r_C}\varphi \tag{A4}$$

For $i>n$, r_i/r_C is a constant (denoted by R) and $L^{(i)}=L^{(i-1)}+\Delta$. Thus, Eq. (A4) becomes

$$\ln\Gamma_i=\ln\gamma_1-\Delta R\varphi \tag{A5}$$

which, like Eq. (A3), is independent of i.

Appendix B: The sedimentation coefficient of spherical (prenuclear) and rod-like (postnuclear) protein aggregates

The sedimentation coefficient of oligomer of dop i, relative to that of monomer, is given by [20]

$$\frac{s_i}{s_1}=\frac{i}{F_i/F_1} \tag{A6}$$

where F_i is the frictional coefficient for sedimentation of species i. It follows from Stokes' law [20] that for a prenuclear oligomer represented as a rigid sphere

$$F_i/F_1=i^{1/3} \tag{A7}$$

The postnuclear oligomer is approximated as a cylindrical rod with radius $r_n=n^{1/3}r_1$, and length/diameter ratio $P_i=L_i+1$, where L is the length/diameter ratio of the cylindrical section of the spherocylindrical model used to calculate the activity coefficient of postnuclear oligomers. According to [24], the frictional coefficient of a randomly oriented cylinder corresponding to an oligomer of dop i, relative to that of spherical monomer, is given by

$$\frac{F_i}{F_1}=n^{1/3}\frac{P_i}{\ln P_i+\varepsilon(P_i)} \tag{A8}$$

where $\varepsilon(P)=0.312+(0.565/P)+(0.10/P^2)$.

References

[1] F. Oosawa, S. Asakura, Thermodynamics of the Polymerization of Protein, Academic Press, London, 1975.

[2] P.D. Ross, A.P. Minton, The effect of non-aggregating proteins upon the gelation of sickle cell hemoglobin, Biochem. Biophys. Res. Commun. 88 (1979) 1308–1314.

[3] W.A. Eaton, J. Hofrichter, Sickle cell hemoglobin polymerization, Adv. Protein Chem. 40 (1990) 63–279.

[4] R.A. Lindner, G.B. Ralston, Macromolecular crowding effects on actin polymerization, Biophys. Chem. 66 (1997) 57–66.

[5] G. Rivas, J.A. Fernandez, A.P. Minton, Direct observation of the enhancement of noncooperative protein self-assembly by macromolecular crowding: indefinite linear self-association of bacterial cell division protein FtsZ, Proc. Natl. Acad. Sci. USA 98 (2001) 3150–3155.

[6] F. Oosawa, S. Higashi, Statistical thermodynamics of polymerization and polymorphism of protein, in: F.M. Snell (Ed.), Progress in Theoretical Biology, 1, Academic Press, New York, 1967.

[7] A.P. Minton, Excluded volume as a determinant of macromolecular structure and reactivity, Biopolymers 20 (1981) 2093–2120.

[8] S.B. Zimmerman, A.P. Minton, Macromolecular crowding: biochemical, biophysical and physiological consequences, Ann. Rev. Biophys. Biomol. Struct. 22 (1993) 27–65.

[9] R.F. Goldstein, L. Stryer, Cooperative polymerization reactions: analytical approximations, numerical examples, and experimental strategy, Biophysical J. 50 (1986) 583–599.

[10] R.C. Chatelier, Indefinite isoenthalpic self-association of solute molecules, Biophys. Chem. 28 (1987) 121–128.

[11] A.P. Minton, Molecular crowding: analysis of effects of high concentrations of inert cosolutes on biochemical equilibria and rates in terms of volume exclusion, Methods Enzymol. 295 (1998) 127–149.

[12] M.A. Cotter, Hard spherocylinders in an anisotropic mean field: a simple model for a nematic liquid crystal, J. Chem. Phys. 66 (1977) 1098–1106.

[13] J.L. Lebowitz, E. Helfand, E. Praestgaard, Scaled particle theory of fluid mixtures, J. Chem. Phys. 43 (1965) 774–779.

[14] J.C. Giddings, E. Kucera, C.P. Russell, M.N. Myers, Statistical theory for the equilibrium distribution of rigid molecules in inert porous networks. Exclusion chromatography, J. Phys. Chem. 72 (1968) 4397–4408.

[15] A. Ogston, The spaces in a uniform random suspension of fibres, Trans. Faraday Soc. 54 (1958) 1754–1757.

[16] I.S. Gradshteyn, I.M. Ryzhik, Table of Integrals, Series, and Products, Academic Press, New York, 1965.

[17] W.H. Press, B.P. Flannery, S.A. Teukolsky, W.T. Vetterling, Numerical Recipes: The Art of Scientific Computing, Cambridge University Press, Cambridge, 1987.

[18] E.T. Adams, M.S. Lewis, Sedimentation equilibrium in reacting systems VI. Some applications to indefinite self-associations, Biochemistry 7 (1968) 1044–1053.

[19] G. Rivas, A. Lopez, J. Mingorance, M.J. Ferrándiz, S. Zorrilla, A.P. Minton, M. Vicente, J.M. Andreu, Magnesium-induced linear self-association of the FtsZ bacterial cell division protein monomer, J. Biol. Chem. 275 (2000) 11740–11749.

[20] C. Tanford, Physical Chemistry of Macromolecules, Wiley, New York, 1961.

[21] T.C. Laurent, The interaction between polysaccharides and other macromolecules. The solubility of proteins in the presence of dextran, Biochem. J. 89 (1963) 253–257.

[22] I.R.M. Juckes, Fractionation of proteins and viruses with polyethylene glycol, Biochim. Biophys. Acta 229 (1971) 535–546.

[23] D.H. Atha, K.C. Ingham, Mechanism of precipitation of proteins by polyethylene glycols: analysis in terms of excluded volume, J. Biol. Chem. 256 (1981) 12108–12117.

[24] J.G. Garcia de la Torre, V.A. Bloomfield, Hydrodynamic properties of complex, rigid, biological macromolecules: theory and applications, Q. Rev. Biophys. 14 (1981) 81–139.